© 2021. Published by The Company of Biologists Ltd | Journal of Cell Science (2021) 134, jcs258382. doi:10.1242/jcs.258382

RESEARCH ARTICLE

Precise regulation of presenilin expression is required for sea urchin early development

Odile Bronchain[1], Laetitia Philippe-Caraty[1,*], Vincent Anquetil[2] and Brigitte Ciapa[1,‡]

ABSTRACT

Presenilins (PSENs) are widely expressed across eukaryotes. Two PSENs are expressed in humans, where they play a crucial role in Alzheimer's disease (AD). Each PSEN can be part of the γ-secretase complex, which has multiple substrates, including Notch and amyloid-β precursor protein (AβPP) – the source of amyloid-β (Aβ) peptides that compose the senile plaques during AD. PSENs also interact with various proteins independently of their γ-secretase activity. They can then be involved in numerous cellular functions, which makes their role in a given cell and/or organism complex to decipher. We have established the *Paracentrotus lividus* sea urchin embryo as a new model to study the role of PSEN. In the sea urchin embryo, the *PSEN* gene is present in unduplicated form and encodes a protein highly similar to human PSENs. Our results suggest that PSEN expression must be precisely tuned to control the course of the first mitotic cycles and the associated intracellular Ca^{2+} transients, the execution of gastrulation and, probably in association with ciliated cells, the establishment of the pluteus. We suggest that it would be relevant to study the role of PSEN within the gene regulatory network deciphered in the sea urchin.

KEY WORDS: Presenilin, PSEN, Sea urchin, Development, Mitosis, Calcium

INTRODUCTION

Presenilins (PSENs) are transmembrane proteins that play both proteolysis-dependent and -independent functions in the cell (Duggan and McCarthy, 2016; Otto et al., 2016). Two PSENs are expressed in vertebrates, PSEN1 and PSEN2. Particular attention has been paid to these proteins since the identification, more than 20 years ago, of *PSEN1* mutations that are associated with the earliest familial forms of Alzheimer's disease (AD). Familial AD (FAD) represents ∼2% of all AD cases, with the remaining cases being 'sporadic' and mostly linked to aging (Lanoiselée et al., 2017; Xia, 2019). PSENs are cleaved into N-terminal (Nter) and C-terminal (Cter) fragments that form the enzymatic active site of the γ-secretase complex (Oikawa and Walter, 2019). This complex cleaves the amyloid-β precursor protein (AβPP), producing amyloid-β (Aβ) peptides, which form aggregates that are deposited extracellularly as amyloid or senile plaques during AD (Wolfe, 2019). Around 100 other proteins have been identified so far as γ-secretase substrates, and besides AβPP, most of them are type-I transmembrane proteins, such as Notch (Duggan and McCarthy, 2016; Parks and Curtis, 2007; Haapasalo and Kovacs, 2011). Notch plays a key role in a range of very different contexts, including diseases such as cancer and embryonic development (Collu et al., 2014; Bray, 2016). For example, Notch is essential for the formation of somites, the embryonic precursors of the vertebrae, ribs and other adult structures (Wahi et al., 2016). Therefore, one can speculate that PSENs have a determinant role during development that is Notch-dependent.

An abundant literature describes studies that have been carried out in multiple model systems – from *in vitro* assays, through cell cultures, to mouse or rat models expressing numerous mutated PSENs (Duggan and McCarthy, 2016; Oikawa and Walter, 2019). These studies have shown that PSENs can also interact, independently of γ-secretase activity, with a variety of proteins, including BCL-2, β-catenin, GSK3β and ubiquitin. They are involved in apoptosis, cell signaling, synaptic function and transcription, among other functions (Parks and Curtis, 2007; Duggan and McCarthy, 2016). In particular, PSEN2 interacts with mediators of intracellular free Ca^{2+} (Ca_i) homeostasis such as SERCA pumps, inositol trisphosphate (IP_3) and ryanodine receptors (Duggan and McCarthy, 2016). This role in Ca_i homeostasis is reinforced by the fact that PSENs carrying FAD mutations alter Ca_i signaling in various *in vitro* assays (Honarnejad and Herms, 2012; Ho and Shen, 2011). In the light of all these results, one might then expect that PSENs have a role as crucial as Notch during development. Indeed, *Psen1*/*Psen2* double-mutant mouse embryos die at day 9 of development with a phenotype closely resembling that of mice with full Notch-1 deficiency (Herreman et al., 1999). It must also be noted that *Psen1*$^{-/-}$ mouse embryos die after birth and show massive loss of neuronal progenitors and neurons, defects in neuronal differentiation and development of the axial skeletal system (Wong et al., 1997). This clearly indicates that *Psen1* expression is linked to neurogenesis, alterations of which in adults would be in part responsible for the cognitive deficits and memory loss that occurs in AD (Hollands et al., 2016).

PSENs or PSEN homologs are expressed in genetically distant species, and the plethora of roles played by these proteins is likely to represent an ancestral function, as suggested by Otto et al. (2016). In *Caenorhabditis elegans*, the PSEN homolog SEL-12 controls Ca_i homeostasis, thus regulating morphology, mitochondrial function and apoptosis (Sarasija and Norman, 2015). In *Drosophila*, the PSEN homolog (Psn) controls the Wnt pathway and the intracellular localization of Notch proteins, and is required for proper neuronal differentiation and associative learning (Guo et al., 1999; Prüßing et al., 2013). The amoeba *Dictyostelium discoideum* contains two PSEN genes, *psenA* and *psenB*, which have partially redundant functions in controlling multicellular development (Otto et al., 2016), cyclic AMP levels and Ca_i release (Ludtmann et al., 2014).

[1]Paris-Saclay Institute of Neuroscience, CNRS, Université Paris-Sud, Université Paris-Saclay, 91405 Orsay, France. [2]Sorbonne Université, Inserm U1127, CNRS UMR 7225, Institut du Cerveau (ICM), F-75013, Paris, France.
*Present address: Institut de Biologie Intégrative de la Cellule (I2BC), Microbiologie Moléculaire des Actinomycètes (MMA), Bâtiment 400, Rue Grégor Mendel, 91400 Orsay, France

‡Author for correspondence (brigitte.ciapa@u-psud.fr)

V.A., 0000-0002-6912-9908; B.C., 0000-0002-3794-6209

Handling Editor: David Glover
Received 7 January 2021; Accepted 24 May 2021

Journal of Cell Science (2021) 134, jcs258382. doi:10.1242/jcs.258382

Given that PSEN proteins are a part of many different signaling pathways, their role in a given cell, tissue or organism is very complex to unravel. Understanding PSEN activity in more simple developing animals may thus help to clarify their role.

The remarkable knowledge of the gene regulatory networks involved in neurogenesis (McClay, 2011; Ben-Tabou de-Leon, 2016) and various events regulating development of the early sea urchin embryo led us to consider the use of this animal as a new model organism to study PSENs. Interestingly, various genes that are involved in neuronal functions in humans are also expressed in sea urchins (Hinman and Burke, 2018). The sea urchin could therefore represent a good model to study the role of PSEN in the development of the nervous system. As demonstrated in other systems, PSEN interacts with β-catenin and GSK3β, which are key components of the Wnt pathway that has been thoroughly investigated in the sea urchin. In the sea urchin, this cascade interacts with that induced by Nodal and BMP2/4 (bone morphogenetic protein), which successively generates the neuroectoderm at the anterior pole of the embryo, the anterior neuroectoderm (ANE) and then the ciliary band (Hinman and Burke, 2018). The role of Notch in the sea urchin is also well characterized, which could help to locate PSEN in the PSEN–Notch context, as explained above. Indeed, in the sea urchin, Notch interacts in successive steps with the Wnt pathway to segregate endomesoderm into separate endoderm and mesoderm fates (Sethi et al., 2012). Notch cooperates with Nodal to control the specification of multipotent progenitors that give rise to the different tissues of the adult after metamorphosis (Materna et al., 2013). Notch also acts as an anti-neural signal by targeting, as does Nodal, the zinc finger homeobox Zfhx1/Z81, which functions during the specification of individual anterior neural precursors and the differentiation of serotonergic neurons (Yaguchi et al., 2012). In sea urchin larvae, Notch represses the expression of the pancreatic and neuronal transcriptional factor Ptf1a in the ciliary band (Perillo et al., 2016). Finally, diverse mechanistic, molecular and ionic aspects that regulate the cell cycle, including Ca_i signaling, have been analyzed in depth in sea urchin embryos (Whitaker, 2008; Costache et al., 2014; Kumar et al., 2015). For instance, our previously published data indicate that levels of Ca_i and of ERK activity control the first mitotic divisions (Ciapa and Philippe, 2013) and cell death fate (Houel-Renault et al., 2013; Philippe et al., 2014) in sea urchin. The control of ERK activity (Dehvari et al., 2008) and Ca_i levels by PSEN in other systems, as mentioned above, appropriately suggests a role in cell cycle progression. For these reasons, we have investigated the role of the single PSEN, highly similar to that of humans, that is expressed in the sea urchin *Paracentrotus lividus*. Our results suggest that PSEN controls different steps of early development, from the first mitotic cell cycles through gastrulation and at least to the pluteus larva stage.

RESULTS

Expression of PSEN changes during the first two mitotic cycles

Clones of PSEN transcripts can be found in cDNA libraries deposited in the *P. lividus* database (http://octopus.obs-vlfr.fr) that have been generated either from unfertilized eggs (Pl EGG) or at the gastrula or pluteus stage (Pl GASPLU). A single *PSEN* gene is expressed at these stages. The *P. lividus* PSEN cDNA clone that we used in this study contains a stop codon at position 1106 (Table S2). We do not know the origin of this point mutation. The translated *P. lividus* PSEN protein (without taking into account this stop codon) contains 507 amino acids, with an expected molecular mass of around 56.7 kDa (calculated using https://web.expasy.org), which is slightly higher than that of human PSENs (Fig. 1). This protein contains domains that are highly similar to those of the two human PSENs, PSEN1 and PSEN2 (Fig. 1). In particular, the nine transmembrane domains (TM1–TM9), the endoproteolytic cleavage site, the catalytic sites and the domain that allows recognition by nicastrin (NCT), a protein of the γ-secretase complex, are particularly well conserved between the two species (Fig. 1). Notably, the N-terminal end and a large domain of the cytosolic loop located between the transmembrane domains TM6 and TM7 are notably divergent between human and *P. lividus* PSENs, as is also observed when comparing sea urchin PSEN sequences from *P. lividus* and *Strongylocentrotus purpuratus* (Fig. S1).

Western blotting performed on extracts of unfertilized eggs using an antibody raised against a peptide from the Nter region of *P. lividus* PSEN (anti-NterPSEN) allowed the detection of three bands at 48, 35 and 15–16 kDa. These bands all disappeared

Fig. 1. The *P. lividus* PSEN sequence. Comparison of *P. lividus* PSEN with human (*Homo sapiens*) PSEN1 (NM_007318) and PSEN2 (NM_000447). Alignment of amino acid sequences was performed using the Clustal Omega program (https://www.ebi.ac.uk/Tools/msa/clustalo/), and positions are labeled with Clustal Omega consensus symbols. The transmembrane domains (TM1–TM9) are indicated (dashed lines). The large region between TM6 and TM7 is a cytosolic loop where the endoproteolytic cleavage site (red) is located. The catalytic sites (green) and the domains that allow recognition by nicastrin (NCT), APH1 and PEN2 are shown.

Journal of Cell Science

Journal of Cell Science (2021) 134, jcs258382. doi:10.1242/jcs.258382

with increasing concentrations of the immunogen TA-24 peptide (Table S1, Fig. S2), confirming the specificity of this antibody. A commercial antibody raised against the Cter region of human PSEN1 (anti-CterPSEN) detected two main bands at 20 and 42 kDa (Fig. 2A, panel b) the intensity of which also declined in the presence of increasing concentrations of the related immunogen peptide (Fig. S2). A timecourse after fertilization of PSEN expression using both antibodies in western blot analysis was then performed on three different batches of eggs, giving similar results. Western blots from a representative batch are shown in Fig. 2A and are quantified in Fig. 2B. A peak of expression was detected at ∼50 min after fertilization, the time when most embryos are at anaphase, by using either the anti-NterPSEN antibody (Fig. 2A, panel a; Fig. 2B, panels a and c) or the anti-CterPSEN (Fig. 2A, panel b; Fig. 2B, panels b and c). These results suggest that the production of Nter and Cter fragments of PSEN changes during mitosis. This leads to the question of whether this event is linked to cell cycle progression.

PSEN controls the first mitotic divisions

The origin of the PSEN Nter and Cter fragments is not yet clearly elucidated. PSEN could be cleaved by a yet-to-be-discovered presenilinase or by autoproteolysis. The latter mechanism is currently the most accepted hypothesis (Brunkan et al., 2005). Therefore, we first looked for a way to test whether endoproteolysis of PSEN controls the first mitotic divisions.

To our knowledge, no specific inhibitor of the PSEN cleavage has been found. In a first set of experiments, we reasoned that a peptide corresponding to the endoproteolytic domain of PSEN (as described in the Materials and Methods section) would act as a competitive inhibitor of a putative enzyme responsible for this cleavage. However, injection of increasing amounts of such a peptide (up to 100 µg/ml) before fertilization had no effect on early development, at least until the blastula stage that was normally reached (data not shown). In a second set of experiments, we tested whether inhibition of γ-secretase activity using DAPT affected cell cycle progression, since some γ-secretase inhibitors can reduce PSEN endoproteolysis (Beher et al., 2001; Campbell et al., 2002). DAPT used at 8 µM is indeed known to alter neurogenesis in the sea urchin when added after the blastula or gastrula stages (Materna et al., 2013; Garner et al., 2016), but whether it affects earlier times of development had not been tested. The addition, 5 min after fertilization, of increasing concentrations of this drug to the culture medium did not alter division even at the highest concentration tested (20 µM, data not shown). The lack of effect was not due to a low permeability of the plasma membrane to the drug since its direct injection in the egg before fertilization led to the same results (Fig. S3). Taken together, these results suggest that if PSEN cleavage controls the first mitotic divisions, the involved mechanism is likely independent of γ-secretase activity.

We next tested whether the two anti-PSEN antibodies could be used as blocking agents. Microinjections of increasing concentrations of each of them were performed before sperm addition and egg fertilization. In our first test experiment, we tested each antibody at a similar concentration (100 µg/ml). None of the embryos injected with the anti-CterPSEN antibody (14 injected in total) divided, whereas all embryos injected with the anti-NterPSEN antibody divided (12 injected in total). We then repeated this experiment in two different females with the anti-CterPSEN antibody used at this same concentration (100 µg/ml) but with a twofold dilution of the anti-NterPSEN antibody stock (0.8 mg/ml). All embryos injected with anti-NterPSEN antibody divided (9 and 8 in each experiment, 17 total), whereas almost all those injected with the anti-CterPSEN antibody (11/12 and 13/15 in each experiment, 24/27 total) did not divide. Typical images are shown in Fig. 3A. Since the anti-NterPSEN antibody had no effect, despite

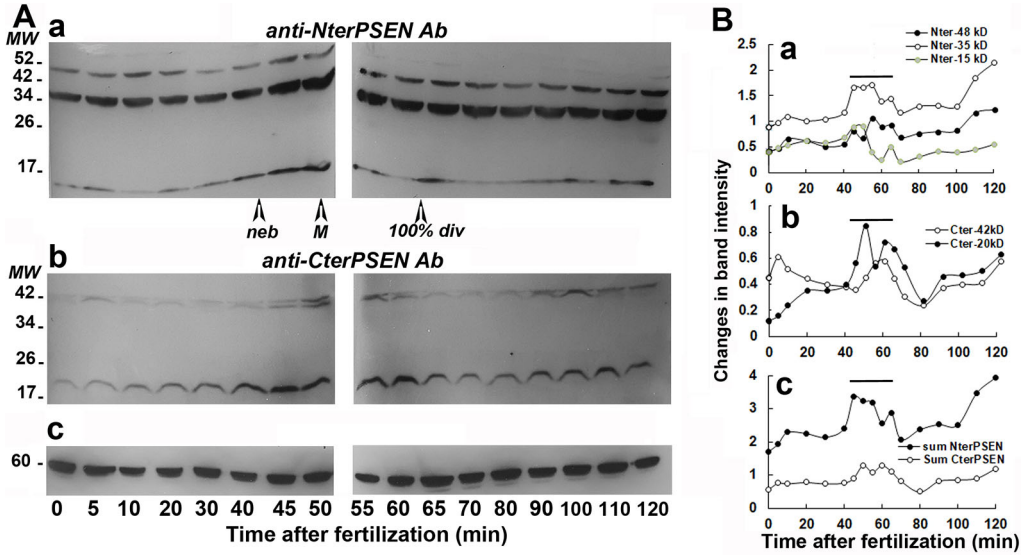

Fig. 2. Timecourse of PSEN expression after fertilization. (A) Western blotting and (B) quantification performed using the same extracts from *P. lividus* eggs for each blot and either the anti-NterPSEN antibody (panel a), the anti-CterPSEN antibody (panel b) or an anti-α-tubulin antibody, which was used as loading control (panel c). The anti-NterPSEN antibody detects three bands, while the anti-CterPSEN antibody detects two bands (MW, molecular mass in kDa). The first embryos enter mitosis (nuclear envelope breakdown, neb) at 42 min after fertilization, the first embryos showing a metaphase spindle (M) are seen at 55 min and all embryos have divided (100% div) at 65 min after fertilization. (B) Quantification of bands detected by western blotting was performed as explained in the Materials and Methods. Quantification of individual bands detected by the anti-NterPSEN antibody (48 kDa, 35 kDa and 15 kDa) and anti-CterPSEN antibody (42 kDa and 20 kDa) are shown in panels a and b, respectively. The sum of intensities for the bands detected by the anti-NterPSEN and anti-CterPSEN antibodies are shown in panel c, illustrating that the expression peaks of the Nter and the Cter fragments are remarkably coordinated and occur at the time of mitosis (indicated by the bold horizontal lines). Data shown are representative of three independent experiments.

Journal of Cell Science (2021) 134, jcs258382. doi:10.1242/jcs.258382

being almost ten times more concentrated than the anti-CterPSEN antibody, it is likely that the latter has a very deleterious and a significant effect compared to that of the anti-NterPSEN antibody.

We next tested whether these conditions altered the Ca_i transients that normally occur at the time of fertilization, pronuclear migration and cytokinesis, as seen in non-injected embryos (Fig. 3B, panel a) and as previously reported (Tosca et al., 2012). These Ca_i peaks were recorded in most embryos injected with the anti-NterPSEN antibody before fertilization (Fig. 3B, panel a). In contrast, almost all embryos injected with the anti-CterPSEN antibody showed only the first fertilization Ca_i peak but not the following mitotic peaks (data from three of these embryos are shown in Fig. 3B, panel b). This effect is likely specific, since injection of the anti-NterPSEN antibody had no effect on this early mechanism. These results strongly suggest that the Cter fragments of PSEN may act on Ca_i signaling and mitotic cycle mechanisms.

Finally, the role of PSEN synthesis was evaluated using a morpholino (MO)-based knockdown strategy. It is well known that the rate of protein synthesis is very low in unfertilized eggs and is stimulated after fertilization (Colin and Hille, 1986). Altering the maternal stock of any protein before fertilization is therefore difficult, but *de novo* synthesis can be blocked from fertilization onward.

Injection of increasing concentrations of an MO targeting PSEN (PSEN-MO), up to 200 µM, before sperm addition did not affect the first mitotic divisions until the four to eight-cell stage (Fig. 3C, MO panel a), a clear delay in divisions being observed when control embryos are at the 16-cell stage (Fig. 3C, MO panel b). Although we cannot rule out that the MO did not affect the PSEN early expression, these results suggest that the stock of PSEN already present in the unfertilized egg is sufficient to allow progression of development up to this stage. This stock most probably declines with time, as indicated by the delay in embryo division after the eight-cell stage. After the 16-cell stage, development was severely altered, as described below. Injection of a control MO had no effect (data not shown).

MO-mediated loss-of-function experiments performed at later times of development require the use of PSEN mRNAs that are insensitive to the MO in order to rescue the effect of the MO. The *P. lividus* PSEN cDNA clone that we used contains a stop codon at position 1106, just after the sequence encoding the endoproteolytic domain (Fig. 1), and would produce a truncated protein containing only an intact Nter fragment. We therefore made constructs to produce the following: (1) mRNA made from the original clone and sensitive (WtRNA) or made resistant (WtrRNA) to the MO, which

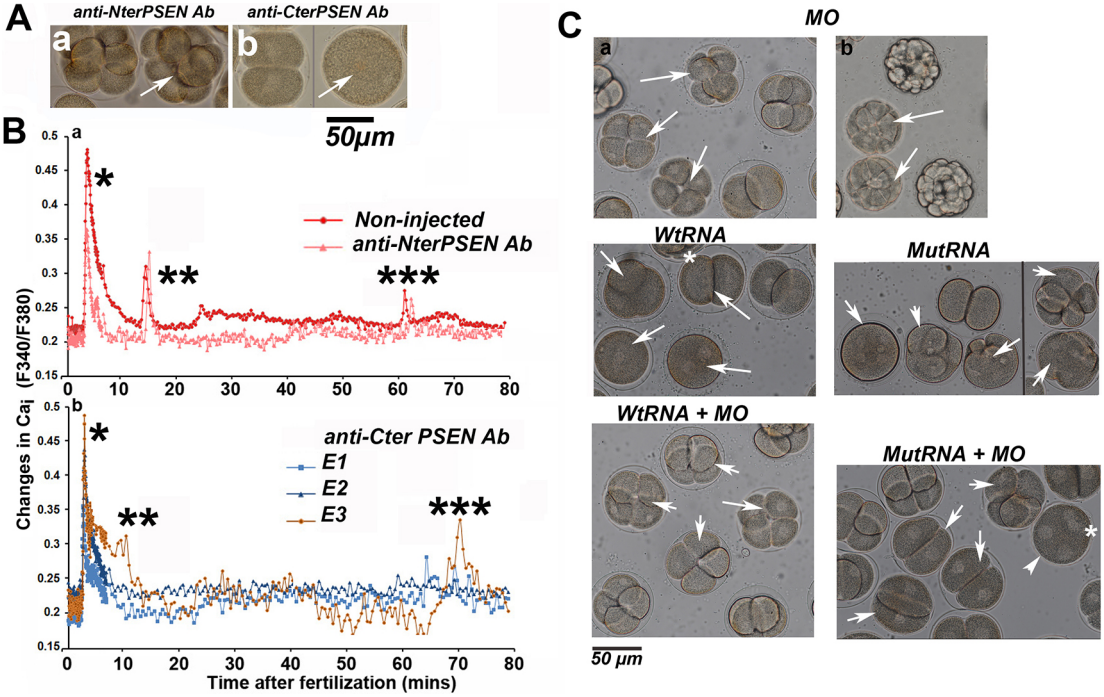

Fig. 3. Role of PSEN during mitosis. (A) Observation by microscopy of embryonic development after injection of anti-PSEN antibodies (Ab) prior to fertilization. Injected embryos are indicated by an arrow and were identified using a co-injected green fluorescence marker (Fig. S3). After injection with anti-Nter PSEN antibody (panel a), all embryos divided (17 injected from two different females). After injection with anti-Cter PSEN antibody (panel b), a very rapid arrest of development occurred (24 out of 27 total injected embryos from two different females), one such non-divided embryo is shown on the right. The vertical line indicates a join between two areas of the same image. (B) Timecourse of Ca_i changes after fertilization. Following injection of the anti-NterPSEN antibody (panel a, pink), Ca_i peaks that are normally seen in non-injected embryos (red) just after sperm addition (*) and at the time of pronuclei migration (**) and cytokinesis (***) were recorded in 11 out of 13 total embryos injected with antibody before fertilization. Following injection of the anti-CterPSEN antibody (panel b), the first fertilization Ca_i peak (*) but not the following mitotic peaks (** and ***) were normally detected in 14 injected embryos out of 17 embryos from three different females. Records of three different embryos (E1, E2 and E3) are shown. Ca_i changes are shown as the ratio of the fluorescence intensities measured at 340 nm excitation (F340) and 380 nm (F380). (C) Observation by light microscopy of the first mitotic divisions after modifications of PSEN expression. Injected embryos are indicated by arrows, and were identified using a co-injected green fluorescence marker (Fig. S4). All non-injected embryos divided normally in each experiment, and all embryos injected with the PSEN MO (top; 158 total, 8 females) divided normally until the four-cell stage (panel a) but with a delay after the eight-cell stage (panel b). Injection of embryos from two different females with WtRNA (middle left; 21 total) or MutRNA (middle right; 34 total) induced aberrant or no cleavage, resulting in mostly polynuclear embryos except in four embryos injected with WtRNA that divided normally (*). Embryos injected with MO and WtRNA (lower left; 26 total) divided normally. Those injected with MO and MutRNA (lower right) either divided, although more slowly than the non-injected embryos (22 embryos), or not (7 embryos; *). Vertical line in the MutRNA panel indicates a join between two areas of the same image.

Journal of Cell Science (2021) 134, jcs258382. doi:10.1242/jcs.258382

should lead to the production of a truncated protein lacking the Cter region; (2) mRNA where this point mutation is modified (see Materials and Methods) allowing the expression of a full-length protein and either sensitive (MutRNA) or resistant (MutrRNA) to the MO. We first tested each of the mRNAs at 0.15 µg/µl, which is the usual RNA concentration used in our previous experiments (Bronchain et al., 2017) and used by others to perform rescue experiments in sea urchins (Duboc et al., 2004). However, we were puzzled to observe that all embryos (12–19 injected embryos per mRNA) did not divide properly in these conditions. Both WtRNA and MutRNA induced aberrant or no cleavage, resulting in polynuclear embryos, and only rare normally divided embryos could be seen after injection with WtRNA (Fig. 3C, middle panels).

In order to test whether the effects on division triggered by 0.15 µg/µl mRNA treatment were specific, we co-injected 150 µM PSEN-MO to titrate the effect of each mRNA. In these conditions, most embryos injected with WtRNA and MO divided normally (Fig. 3C, lower left panel). Embryos injected with MutRNA and MO either divided (although more slowly than the non-injected embryos) or not (Fig. 3C, lower right panel). Injection of the MO-resistant RNAs (WtrRNA and MutrRNA) alone triggered aberrant divisions like those observed with the corresponding MO-sensitive RNAs, but the effects could not be prevented by MO co-injection (data not shown). It is likely that the abnormal divisions induced by mRNA injection were due to an excess of PSEN synthesis and not non-specific effects induced by the mRNA itself because the effects of the MO-sensitive mRNA could only be canceled by the MO. Taken together, these results suggest that the level of PSEN, and more particularly that of Cter part of the protein, must not be in excess during mitosis.

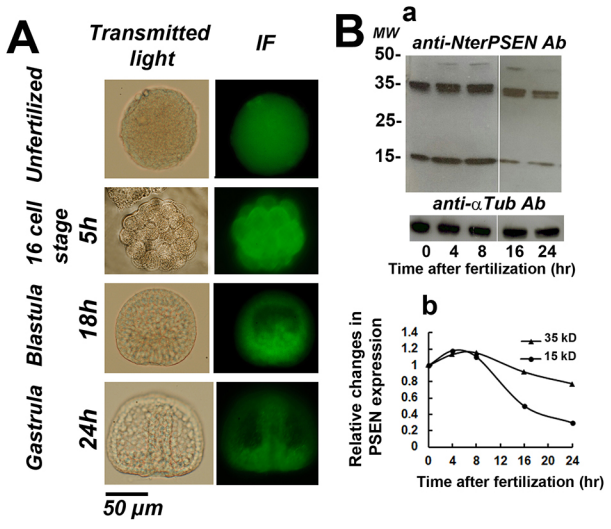

Fig. 4. Expression of the PSEN protein during development. (A) Transmitted light (left panels) and IF images after labeling with the anti-NterPSEN antibody (right panels) showing unfertilized eggs and 16 cell-stage, blastula-stage and gastrula-stage embryos. The control experiment with secondary antibody only did not give any signal (data not shown). PSEN is uniformly expressed in the unfertilized egg, while a higher level of expression is observed at the vegetal side in the 18 h blastula and the 24 h gastrula. (B) Timecourse during development of PSEN expression as determined by western blotting (panel a) and quantification (panel b) performed using the same anti-NterPSEN antibody (Ab), with anti-α-tubulin shown as loading control (MW, molecular mass in kDa). Three PSEN bands are seen, as explained in Fig. 2, the intensity of which starts to decrease after 8 h of development. Quantification of the 35 kDa and the 15 kDa bands (panel b) is performed as explained in the Materials and Methods. Data shown in A and B are representative of three experiments.

PSEN is expressed in endomesoderm at gastrulation stage

The γ-secretase activity of PSEN targets various substrates, one of which is Notch. Given that Notch plays a key role in the segregation of mesoderm from endoderm and in the specification of the secondary mesenchyme cells (SMCs) (Sherwood and McClay, 2001), we studied the expression of PSEN during early development. Results of immunofluorescence (IF) staining using the anti-NterPSEN antibody are displayed in Fig. 4A. We observed that PSEN was first uniformly expressed in the unfertilized egg until at least the 16-cell stage, and then appeared more concentrated on the vegetal side of the 18 h blastula embryo, namely in the endoderm and mesoderm territories, including the primary mesenchyme cells (PMCs) (McClay, 2011). These territories also expressed PSEN in the 24 h gastrula, thus giving a heavy staining at the periphery of the archenteron, in PMCs and SMCs. Similar results were obtained using the anti-CterPSEN antibody, although the staining appeared more diffuse and less intense than that obtained with the anti-NterPSEN antibody (data not shown). Analysis of western blots using the anti-NterPSEN antibody showed that PSEN expression dramatically decreased after the first 3–4 mitotic cycles to reach a low level at the blastula stage, after which it remained more or less constant until the gastrula stage (Fig. 4B).

Our results show that *PSEN* transcription and expression of the PSEN protein follow similar kinetics until the blastula stage. The IF results reported above corroborate those obtained by whole-mount *in situ* hybridization studies (WISH) using a DAB staining protocol. The *PSEN* antisense probe gave signal as follows: unfertilized eggs were faintly and uniformly labeled, the 18 h blastula was entirely stained but appeared more intensely stained in the endomesodermic half, and a very strong staining was seen around the blastopore, midgut, hindgut, PMCs and SMCs of the 24 h gastrula (Fig. 5A). Results obtained by reverse transcription PCR (RT-PCR; Fig. 5B)

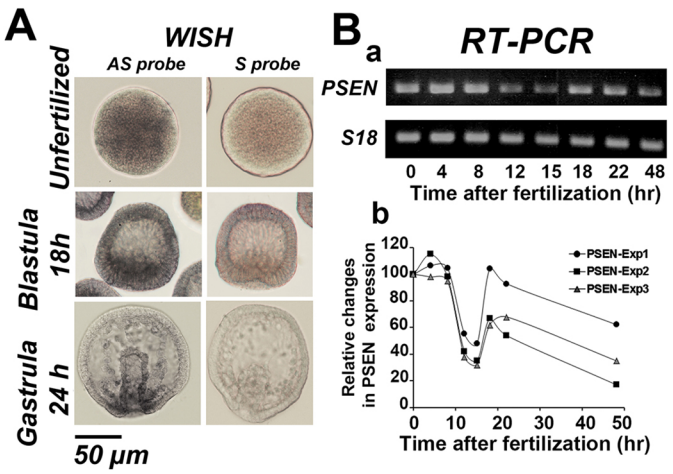

Fig. 5. *PSEN* transcription during development. (A) WISH labeling of embryos arrested before (unfertilized) and 18 h (blastula) or 28 h (gastrula) after fertilization. The *PSEN* antisense (AS) probe gave a signal while no signal was detected in this experiment with the sense (S) probe. Unfertilized eggs are faintly and uniformly labeled, whereas the 18 h blastula is more intensely stained in the endomesodermic half and the 24 h gastrula is strongly stained around the blastopore and in the area of the PMCs. (B) Semi-quantitative RT-PCR (panel a) and quantification (panel b) of *PSEN* expression in three similar experiments (Exp1–3). Expression of *S18* is used as an internal control. *PSEN* expression decreases 8 h after fertilization to reach a low level at the blastula stage (~12–15 h). A burst of expression occurs when embryos gastrulate (~20–24 h) with an amplitude that varies with the batch of embryos (Exp1–3).

Journal of Cell Science (2021) 134, jcs258382. doi:10.1242/jcs.258382

revealed that *PSEN* expression started to decrease 8–10 h after fertilization to reach a low level at the blastula stage, after which it was transiently stimulated before decreasing again until gastrula stage. In conclusion, PSEN is first expressed in the whole early embryo and becomes more and more confined during embryonic development until expression is restricted to the midgut, hindgut, the PMCs and the SMCs of the late gastrula.

PSEN is mostly expressed around the digestive system of the pluteus

We progressed our investigation to the pluteus stage. IF staining of 48 h embryos with the anti-NterPSEN antibody indicated that PSEN is mostly expressed in cells scattered around the digestive system (Fig. 6). At this stage, isolated stained cells were embedded in the stomach epithelium and throughout the stomach, around the esophagus, as well as in the mouth, the right coelom and the intestine. The anti-CterPSEN antibody did not give any signal at this time of development despite the use of various protocols for IF staining (data not shown). PSEN expression thus seems to mirror that of Notch, which is known to be essential for the embryonic development of the gut in sea urchins (Perillo et al., 2016) and in various other species including amphioxus (Holland et al., 2001) and mouse (Schröder and Gossler, 2002).

We therefore asked whether PSEN could also have a role in neural differentiation (Walton et al., 2006). Neurogenic capacity in the sea urchin embryo is initially present throughout the entire ectoderm and later becomes restricted to the ANE and the ciliary band neuroectoderm (CBE) (Slota et al., 2020). We performed triple stainings using Hoechst 33258, the anti-NterPSEN antibody and an anti-acetylated tubulin antibody that is commonly used to visualize the ciliary band of the sea urchin (Wood et al., 2018). Confocal images of one such labeled pluteus is shown in Fig. 7. As described above, cells expressing PSEN were mostly found around the digestive system. Although some of these cells were obviously not labeled with the anti-acetylated tubulin antibody, irrespective of the observation focus, most also expressed acetylated tubulin. A few other cells expressing PSEN but not acetylated tubulin were also seen in the posterior part of the embryo. Finally, a faint PSEN staining coupled to that of acetylated tubulin could be detected in the ciliary band. In conclusion, most cells that express PSEN seem to be ciliated cells at the pluteus stage.

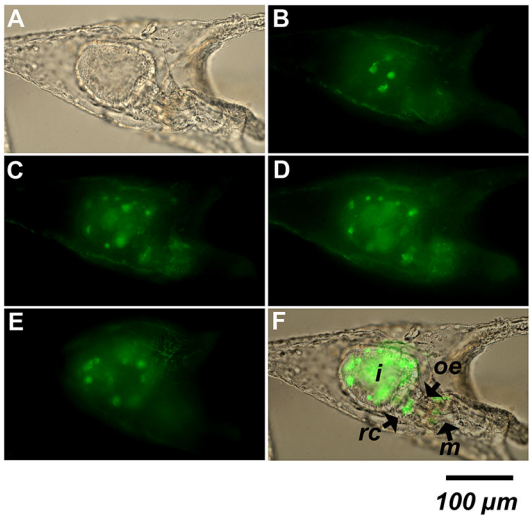

Fig. 6. Expression of PSEN in the pluteus. Observation of a pluteus following IF staining with the anti-NterPSEN antibody. The transmitted light image (A) and the epifluorescence images obtained at different focal planes (B–E) are shown as a merged image in F. At this stage, isolated stained cells are embedded in the stomach epithelium and throughout the stomach, around the esophagus (oe), the mouth (m), the intestine (i) and the right coelom (rc). Seven plutei were imaged, giving similar results.

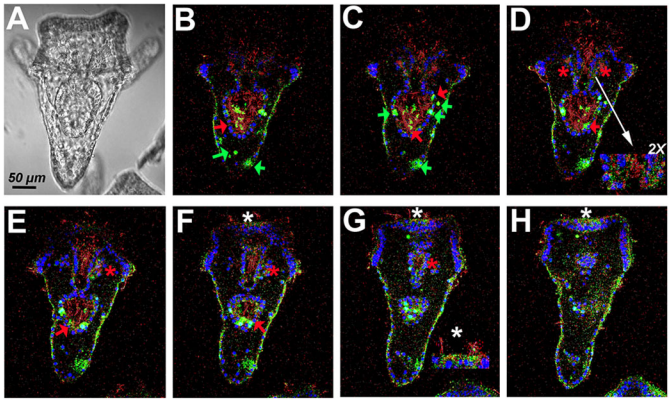

Fig. 7. Co-expression of PSEN with acetylated tubulin. Transmitted light image (A) and confocal fluorescence images (B–H) of one pluteus (representative of five analyzed plutei) stained with Hoechst 33258 (blue), anti-NterPSEN antibody (green) and anti-acetylated tubulin antibody (red). Cells expressing PSEN are found isolated and embedded in the stomach epithelium and throughout the stomach, around the sphincter and the esophagus, and in the upper lip of the mouth. Some cells are clearly either double stained for PSEN and acetylated tubulin (red arrows) or only stained for PSEN (green arrows) in images from multiple focal planes. Inset images in D and G show 2× enlargements to highlight the intricate co-labeling of NterPSEN and acetylated tubulin in the esophagus area (red asterisks; inset in D) and the ciliary band (white asterisks; inset in G).

PSEN expression is required for normal embryonic development

Finally, we studied the role of PSEN synthesis during development by using the MO-based strategy and mRNAs made as described above. The results are shown in Fig. 8A–F, and quantification after 24 h of development is presented in Fig. 8G. Normal embryos were observed to be at the blastula stage at ∼12–15 h (Fig. 8A, panel a1), at which time they started to gastrulate and look like ‘small gastrulae’ (Fig. 8A, panel a2). Fully invaginated gastrulae were then observed at 23–26 h (Fig. 8A, panels b1 and b2), after which they elongated until forming plutei 2 days after fertilization (Fig. 8A, panel c). Injection with 150 µM PSEN-MO induced cell death that started after the 16-cell stage. Half of the MO-injected embryos were found dead 24 h after fertilization (Fig. 8G) and less than a third of the population survived 2 days after fertilization. Around a third of the MO-injected population developed to morula stage (Fig. 8B, panel a) and then to blastula stage, with most staying at this stage 24 h after fertilization (Fig. 8B, panels b1–b3; Fig. 8G). These embryos did not significantly develop further but rather started to die, although we observed a few embryos that were clearly gastrulated but were of smaller size and/or without a fully invaginated archenteron (Fig. 8B, panels c1–c3). This rare event occurred with a noticeable delay, since control non-injected embryos observed at the same time were plutei, as shown in Fig. 8A, panel c. Injection of a control MO did not have any effect (data not shown).

We performed rescue and titration experiments with the different *PSEN* mRNAs, as described above. We first tested each of them to assess their individual effect. A preliminary dose-response assay indicated that a concentration of 0.08 µg/ml of each mRNA allowed the best rate of gastrulation when injected individually (data not

Journal of Cell Science (2021) 134, jcs258382. doi:10.1242/jcs.258382

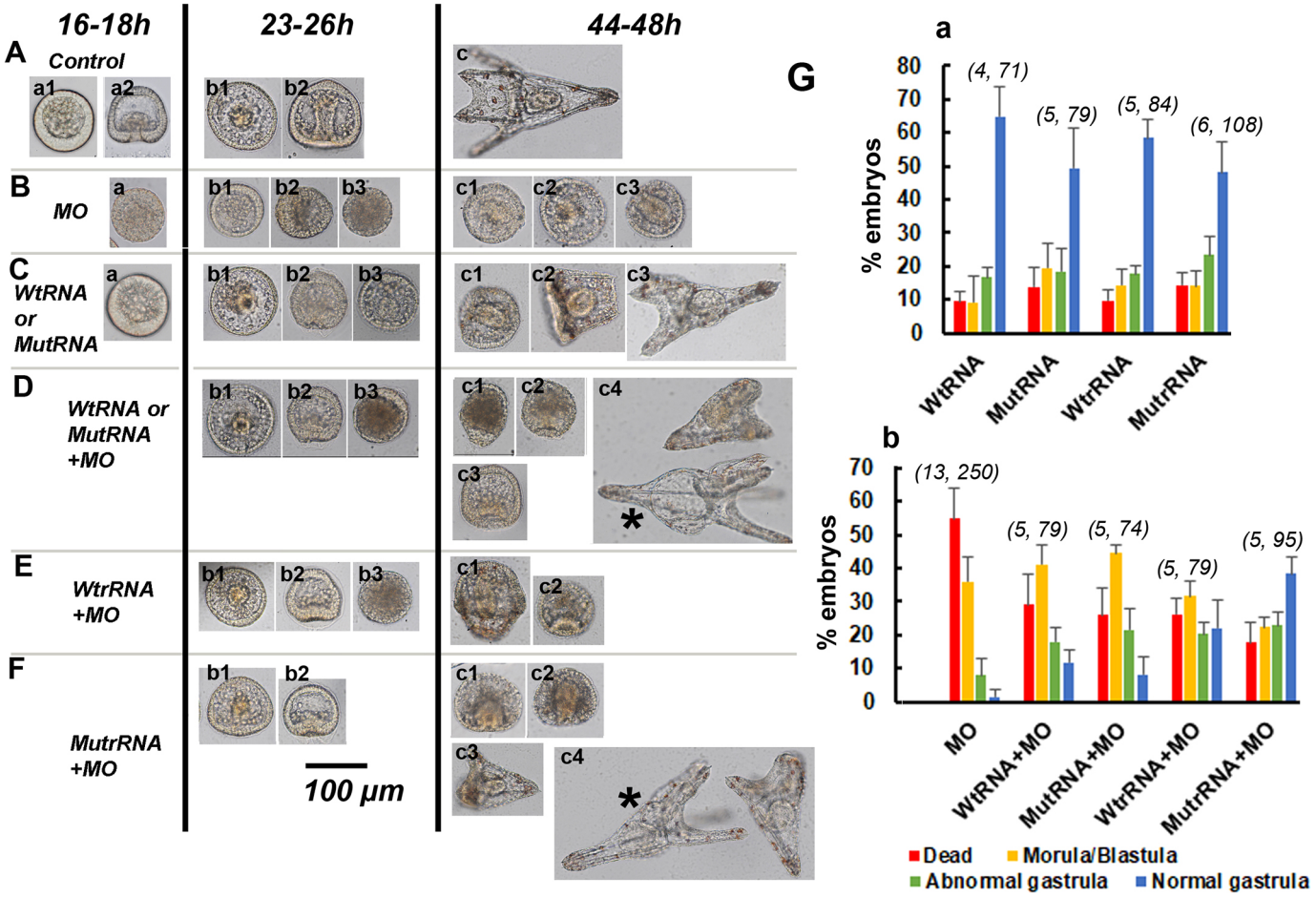

Fig. 8. The role of PSEN expression during embryonic development. (A–F) Typical phenotypes (numbered 1–4) of injected embryos observed by transmitted light microscopy at 16–18 h (a), 23-26 h (b) and 44-48 h (c) after fertilization, times corresponding to the blastula, gastrula and pluteus stages, respectively, of non-injected embryos (control). All injected embryos fluoresce in red (Fig. S5) and description of each phenotype is as given in the text. (A) Control development. Two views of a gastrula; one taken from the side of the archenteron (b1) and one a lateral view (b2) are shown. (B) MO injection. (C) MO-sensitive WtRNA injection. (D) Dual injection of MO with the MO-sensitive WtRNA. (E) Dual injection of MO with WtrRNA, which is resistant to the MO. (F) Dual injection of MO with MutrRNA, which is resistant to the MO. The plutei labeled with a black asterisk (D, panel c4; F, panel c4) are control plutei included for comparison with the treated plutei in the same image, which are smaller in size. (G) Quantification of all results at 24 h of development as percentages of embryos with each phenotype (dead, at morula or blastula stage, or at normal or abnormal gastrula stage). Embryos were injected with each mRNA without (panel a) or with MO (panel b). Data shown are mean±s.e.m. of *n* different females for a total of *N* embryos (as indicated; *n*, *N*) that have divided normally at least once after injection of the different RNAs with or without MO. It must be noted that among the 17 females used in total, each was used to test between one (MO only) and five different conditions that may differ between females. However, for embryos from the same female, the percentage of dead embryos was significantly decreased (two-tailed unpaired Student's *t*-test; $P<0.01$) and the percentage of abnormal or normal gastrula was significantly increased (two-tailed unpaired Student's *t*-test; $P<0.01$) following co-injection of each RNA with the MO, as compared with the values obtained after injection with the MO alone. The percentage of dead embryos and the percentage of normal gastrula following MutrRNA and MO co-injection were significantly decreased and increased (two-tailed unpaired Student's *t*-test), respectively, when compared to those obtained following WtrRNA and MO co-injection in embryos from each of the three common females used to test these two conditions.

shown). We observed that 80–90% of embryos injected with the WtRNA only developed to blastula stage (Fig. 8C, panel a) and then to normal gastrula stage (Fig. 8C, panel b1; Fig. 8G), although 10–20% of them, depending on the batch of embryos used, remained as small early gastrulae even after 24 h of development (Fig. 8C, panels b2 and b3). After 2 days of development, the small gastrulae did not develop further (Fig. 8C, panel c1), while the normal gastrulae either remained at this stage or developed into plutei that were more or less elongated (Fig. 8C, panels c2 and c3). Comparable results were obtained with the corresponding RNA insensitive to the MO, WtrRNA (Fig. 8G). Injection with the MutRNA and its corresponding RNA insensitive to the MO, MutrRNA, gave similar results, although the percentages of successful gastrulation were a little lower than those measured following injection with the WtRNA (Fig. 8G).

Co-injections of the PSEN-MO together with each mRNA were then carried out. A general view of the results indicates that addition of any of the mRNAs to the MO injection reduced the percentage of dead embryos and increased the occurrence of gastrulation in comparison to that recorded after injection of the MO alone (Fig. 8G). We first titrated the effect of the MO by co-injecting with either WtRNA or MutRNA, which are sensitive to the MO. Comparable results were obtained for each mRNA (Fig. 8G). Around 60% of the embryos survived 24 h after fertilization. Rare normal gastrulae were seen (Fig. 8D, panel b1), with most other embryos resembling very small gastrulae (Fig. 8D, panel b2) or remaining at the blastula stage (Fig. 8D, panel b3). At 48 h after fertilization, a third of these embryos were found to be dead, and the surviving embryos had not significantly developed further. The small gastrulae mostly resembled those seen in Fig. 8D, panels c1–c3, and the normal

Journal of Cell Science (2021) 134, jcs258382. doi:10.1242/jcs.258382

gastrulae remained exactly at that same stage, except one that developed into a small pluteus (Fig. 8D, panel c4).

Lastly, we performed experiments to rescue the MO effect by co-injecting with either WtrRNA or MutrRNA, which had been made insensitive to the MO. Co-injection of the MO with WtrRNA gave rates of survival and gastrulation that were very similar to those induced after co-injection with the MO-sensitive mRNA (Fig. 8G). The surviving 24 h embryos either reached gastrula stage (Fig. 8E, panel b1), or resembled blastulae that were invaginated (Fig. 8E, panel b2) or not (Fig. 8E, panel b3). At 48 h, some gastrulae appeared more elongated (Fig. 8E, panel c1), and a few blastulae had developed into small gastrulae (Fig. 8E, panel c2). The MO-insensitive MutrRNA gave the lowest rates of death and the best rates of gastrulation (Fig. 8G). A total of 75% of these co-injected embryos survived 24 h after fertilization, appearing either as normal gastrulae (Fig. 8F, panel b1) or as blastulae that were more or less invaginated (Fig. 8F, panel b2). At 48 h, a few blastulae had become aberrant gastrulae (Fig. 8F, panels c1 and c2), and a few gastrulae had developed into plutei, although these were of a smaller size than that of non-injected control plutei (Fig. 8F, panels c3 and c4). These results strongly suggest that *de novo* synthesis of PSEN is not only required for development but must also be tuned at a critical level in at least two steps: during gastrulation and during the differentiation steps that set up the pluteus larva.

DISCUSSION

Given the multiple properties of PSEN that are either dependent on or independent of γ-secretase activity, it is not surprising that we found the PSEN protein to be involved at various steps of development in the sea urchin.

Only one copy of the *PSEN* gene is expressed in the sea urchin

A single copy of the *PSEN* gene is found in the genome of sea urchins. A recently published evolutionary history study that includes *S. purpuratus* reports that PSEN is represented by two paralogs in vertebrates (PSEN1 and PSEN2), whereas in invertebrate metazoans it is in unduplicated form, with the exception of *C. elegans*, in which presenilin is represented by three paralogs (SEL-12, HOP-1 and SPE-4) (Khan et al., 2020). The authors of this study suggest that presenilins might have their origin in the last common eukaryotic ancestor (LCEA). It is probable that studying PSEN in different model species could lead to new avenues regarding both its catalytic and noncatalytic roles.

PSEN γ-secretase acts during development but does not affect the first mitotic divisions

In the γ-secretase complex, PSEN normally interacts with APH1 (APH1A and APH1B in humans), PEN2 (also known as PSENEN in humans) and nicastrin, all of which are expressed in the sea urchin, although the sea urchin and human homologs of these proteins have a lesser degree of sequence similarity than observed for PSEN (Table S3). The domains allowing recognition of PSEN by these proteins are also well conserved (Fig. 1). Our MO injection experiments and the fact that the γ-secretase inhibitor DAPT alters development after the blastula stage (Ohguro et al., 2011) strongly suggest that one of the means of control exercised by PSEN on development occurs through γ-secretase activity. However, the control of the first mitotic divisions by PSEN is likely to be independent of this activity since neither DAPT treatment nor injection of a peptide corresponding to the endoproteolytic domain of PSEN affected these early times of development.

PSEN endoproteolysis and the role of the Cter and Nter fragments

In humans, the endogenous PSEN exists *in vivo* only as Cter and Nter fragments, and the full-length protein is usually barely detectable (Thinakaran et al., 1996). A 'presenilinase' has not been identified yet, and the accepted dogma is that endoproteolysis is an autocatalytic cleavage event (Brunkan et al., 2005). The expected 37 kDa Nter and 19.5 kDa Cter fragments of the sea urchin PSEN protein that should thus be formed correspond to the main bands detected in our western blotting experiments by the anti-NterPSEN antibody (35 kDa) and the anti-CterPSEN antibody (20 kDa), respectively. The 48 kDa and 42 kDa bands detected by the anti-NterPSEN and anti-CterPSEN antibodies, respectively, could therefore represent the full-length PSEN protein. However, these molecular masses are somewhat smaller than that expected (56 kDa). This could be due to cleavage by endopeptidases at other diverse sites that can be found in the sequence of the sea urchin PSEN (as predicted using https://web.expasy.org/cgi-bin/peptide_cutter/peptidecutter.pl), which could also lead to the production of the 15 kDa band detected by the anti-NterPSEN antibody. As a matter of fact, this hypothesis has been proposed to explain the detection of bands of various sizes in western blots of human PSEN1 and PSEN2 (Mathews et al., 2000).

The Cter and Nter fragments of PSEN have properties of their own. For example, the Cter fragment of PSEN1 associates with β-catenin (Tesco et al., 1998), which via the Wnt pathway controls centrosomal functions, including mitotic spindle formation and centrosome separation (Bryja et al., 2017). The Cter fragment of PSEN2, but not the full-length protein, associates with sorcin, a modulator of the ryanodine receptor (Pack-Chung et al., 2000). These results could explain the arrest of mitosis and the alterations of the mitotic Ca_i transients that we observed in sea urchin embryos after injection of the anti-CterPSEN antibody but not after injection of the anti-NterPSEN antibody. This crucial role of the Cter fragment during mitosis is also illustrated by the fact that an increase in the level of the full-length protein, which was most probably induced after injection of the MutRNA, seems to be more potent to alter mitosis than the increase in levels of the truncated protein lacking the Cter part after injection of the WtRNA. On the other hand, the best scores in rescue experiments were obtained when using the MutrRNA, which allows expression of the full-length protein. It is therefore possible that the Cter fragment of PSEN plays specific roles during development.

Correct expression of PSEN is essential for early development

Critical thresholds of PSEN expression level are obviously required to control different stages of development. How the level of PSEN is regulated in a defined area of the cell or of the embryo is most probably very complex; presenilins are expressed in various intracellular areas including the endoplasmic reticulum (ER), Golgi and cell surface (Area-Gomez et al., 2009; De Strooper et al., 1997; Escamilla-Ayala et al., 2020), where their turnover most probably varies. Too much expression, as triggered after mRNA injection, obviously alters the first mitotic cell division and is clearly harmful for the gastrula, which subsequently develops into the pluteus. On the other hand, too low a level of expression (as triggered by MO injection) is toxic, with half of the MO-injected embryos only reaching the blastula stage, and a critical level of PSEN is clearly required for gastrulation. This latter result was expected since the γ-secretase activity of PSEN cleaves Notch, which is essential throughout gastrulation (Sherwood and McClay,

1999, 2001). Various signaling pathways, including those controlling the cell cycle, rely on a precise control of Ca_i homeostasis. They therefore respond to any stimulation or inhibition of Ca_i release or uptake from or into intracellular compartments (in ER, mitochondria and lysosomes, as well as through the plasma membrane). It is probable that a loss (via injection of MO or antibodies) or gain (via injection of mRNA) of PSEN function both lead to Ca_i alterations and alterations of development. This also probably explains the variable degree of development alteration obtained upon co-injection of the MO and mRNA, whether sensitive to the MO or not, which should give intermediate levels of PSEN between the 'too much' (mRNA alone) and the 'not enough' (MO alone) level.

In the pluteus, cells expressing PSEN are mostly found around the digestive system. At that time of development, the role of PSEN would still complement that of Notch, which acts during endoderm development in *Xenopus* (Contakos et al., 2005), chicken (Matsuda et al., 2005), zebrafish (Kikuchi et al., 2004) and *Drosophila* (Fuss and Hoch, 2002), and which is known to be essential for gut development in amphioxus (Holland et al., 2001) and mouse (Schröder and Gossler, 2002). A few of these PSEN-positive cells appeared to be blastocoelar cells, which are known to be concentrated around the stomach and to mediate the larval immune response (Buckley and Rast, 2017). PSEN could therefore be involved in the differentiation of these immune cells, again probably through Notch, which itself has long been known to be associated with this event (Benson et al., 2004). One can arguably wonder whether PSEN, mainly expressed around the gut, is involved in the development and/or the function of the neural system. This is possible, since PSEN is expressed in areas of the sea urchin embryo that are known to be neurogenic. For example, oral ganglia innervate the lower lips of the mouth, a diffuse network of neural processes overlays the esophagus (Burke et al., 2006), and neurons are found in the intestine and in the anus (Nakajima et al., 2004). Interestingly, pharyngeal neurons that develop *de novo* from the endoderm have been described by Wei et al. (2011). Moreover, cells expressing one or more neuropeptide precursor genes are located around the mouth and in the mid- and fore-gut (Wood et al., 2018), and it would be pertinent to investigate whether these cells are those expressing PSEN. Finally, some of the cells expressing PSEN around the gut were co-labeled with the anti-acetylated tubulin antibody that is commonly used to visualize stable microtubules, including those of primary cilia. Ciliated cells of the gut lumen are involved in the feeding of the larva, and PSEN could be related to the neural control that must necessarily act on the ciliary beating of these cells (Annunziata et al., 2014). We also detected co-labeling for PSEN and acetylated tubulin in the ciliary band, which in the sea urchin is linked to the gut by sensory and motor neurons (Wood et al., 2018). Cilia serve as hubs of cell signaling activity in many organisms, especially during embryonic development (Morris and Vacquier, 2019). Mobile cilia are particularly necessary in sea urchins for Hedgehog signaling (Morris and Vacquier, 2019; Warner et al., 2013). Indeed, Hedgehog and Notch signaling interact together in ciliated cells to influence neuronal specification (Morris and Vacquier, 2019; Kong et al., 2015) and in the gut to regulate the development of the enteric nervous system (Liu and Ngan, 2014). Expression of PSEN in ciliated cells may then well be linked to Notch, the role of which in neural specification and regulation of proneural networks is well characterized in the sea urchin (Burke et al., 2014). This role of Notch is indeed very well conserved from *Drosophila* to humans, being critical in neural stem cell maintenance and neurogenesis in the embryonic brain, as well as in the adult brain (Zhang et al., 2018). Finally, expression of PSEN was seen in the aboral ectoderm in cells that are obviously not ciliated cells. The regulation of oral–aboral ectoderm specification in the sea urchin embryo has been extensively studied in recent years. It would be interesting to study whether PSEN, via the Notch cascade, interferes with the Nodal (Materna et al., 2013) and BMP pathways, which are well known to play a key role in driving the setting of dorsal–ventral patterning in the sea urchin embryo (Floc'hlay et al., 2021) and possibly in all chordates (Su et al., 2019).

In conclusion, it would be relevant to study the role of the *PSEN* gene within the gene regulatory networks of sea urchin species, particularly those networks involving Notch and that control either morphogenesis of the gut (Annunziata et al., 2014) or neurogenesis (Hinman and Burke, 2018). This could help us to understand, for instance, how the regulation of hippocampal adult neurogenesis by PSEN is affected within AD (Hollands et al., 2016). In this regard, the study of PSEN evolution mentioned above (Khan et al., 2020) found that presenilin protein sites that undergo mutations in FAD are highly conserved in metazoans. The authors of this previous study suggest that the involvement of presenilin in AD pathogenicity cannot be ascribed to a single function such as amyloid-β production. It is clear that new approaches and new models could bring new insights to argue against the 'amyloid hypothesis', which seems to be more and more debated (Tse and Herrup, 2017) and has so far led to neither new methods of diagnosis nor novel therapies.

MATERIALS AND METHODS

Handling of gametes and treatment of embryos

Gametes of *Paracentrotus lividus* were collected, prepared and fertilized in artificial sea water (ASW; Reef Crystals Instant Ocean), as described previously (Philippe et al., 2014). The γ-secretase inhibitor *N*-[*N*-(3,5-difluorophenacetyl)-L-alanyl]-S-phenylglycine t-butyl ester (DAPT) was dissolved in DMSO and used at a final concentration of 8 µM.

For western blotting or semi-quantitative RT-PCR analysis, samples of eggs and embryos were taken before or at different times after fertilization and treated as previously described (Philippe et al., 2014; Ciapa and Philippe, 2013) to obtain dry pellets that were frozen at −80°C until analysis. For immunofluorescence labeling or *in situ* hybridization experiments, eggs were fertilized in the presence of 1 mM ATAZ (3-amino-1,2,4-triazole; Sigma) to prevent hardening of the fertilization membrane. At 2 min after fertilization, eggs were diluted ten times in ASW and quickly filtered several times through an 85 µm filter to remove fertilization membranes. Decanted embryos were rinsed twice in ASW and then left to develop in ASW until arrest at various times post fertilization. Samples were diluted twice in ASW containing 8% paraformaldehyde (PFA) and left for fixation for 1 h in this medium. Embryos were then rinsed once by decantation with TBS (Tris-HCl 10 mM, NaCl 150 mM, pH 7.4) and finally taken up in TBS and glycerol (1:1) where they were kept at −20°C until use.

Western blotting

Dry egg pellets were dissolved in sample buffer [SB: 40% glycerol, 2% SDS, 0.05% Bromophenol Blue and 100 mM dithiothreitol (DTT)] and heated to 95°C. Proteins were separated using SDS–PAGE. Western blotting and dilutions of all antibodies were performed as previously described (Zhang et al., 2005; Ciapa and Philippe, 2013) using the following antibodies: (1) an anti-NterPSEN antibody (1:1000), made in rabbit immunized against a peptide (TA-24; see sequence in Table S1) located in the Nter part of the *P. lividus* PSEN sequence (Proteogenix SAS, France); (2) a commercial anti-CterPSEN antibody (1:1000; anti-presenilin 1; C-20; sc-1244; Santa Cruz Biotechnology) with associated blocking peptide sc-1244 P (Santa Cruz Biotechnology); and (3) a mouse anti-α-tubulin antibody (1:2000; CP06; Calbiochem). Bands were quantified using ImageJ (NIH, Bethesda, MD), normalized by comparison to the α-tubulin signal

and then expressed relative to the value determined in control eggs or embryos, which was arbitrarily taken as one.

PSEN immunostaining

Fixed eggs and embryos were rinsed in TBS containing 2% Triton X-100 (TBS-T), and labeling was performed as described previously (Zhang et al., 2005) using the anti-NterPSEN antibody (1:500) with an anti-rabbit IgG FITC-conjugated secondary antibody (Jackson), and an anti-acetylated tubulin antibody (1:1000; a gift from Ina Arnone, Stazione Zoologica di Napoli, Naples, Italy) with an anti-mouse IgG rhodamine-conjugated secondary antibody (Jackson). For Hoechst staining, embryos were incubated for 30 min with 5 µg/ml Hoechst 33258 (Polysciences) and rinsed again three times with TBS-T.

Transmitted light images and fluorescence images were taken using a Nikon D600 after observation by epi-fluorescence with a Nikon Eclipse TE300 equipped with a 20× Plan Fluor Nikon objective. Confocal microscopy analysis was performed using a Zeiss LSM 700 and a 40× objective. Stacks of images taken every 3 µm were acquired on the entire depth of the embryo.

Whole-mount *in situ* hybridization

To obtain a *PSEN* probe for whole-mount *in situ* hybridization (WISH), we used a clone (SPOACLEB43YL17) from a *P. lividus* cDNA library (http://octopus.obs-vlfr.fr). The translated sequence of the insert, initially in the pSPORT-Sfi vector, was transferred to pBluescript II KS+ using the pair of primers PSENpBl-Fw and PSENpBl-Rv. All primers and sequences are given in Table S1 and Table S2, respectively.

DIG-labeled WISH probes were synthesized using Hind III/T7 RNA polymerase for the sense probe (negative control) and BamH1/T3 RNA polymerase for the antisense probe (to detect *PSEN* sense RNA) and were labeled using digoxigenin-11-UTP (Roche). WISH was performed on fixed embryos following a protocol described by Duboc et al. (2004).

Semi-quantitative RT-PCR

Total RNA was purified from dry pellets of embryos using an RNeasy Plus Micro Kit (Qiagen) following the manufacturer's protocol. 1 µg RNA of each sample was reverse transcribed using the SuperScript II RT kit (Invitrogen) and 0.2 µM reverse primers (PSEN-Rv and S18rt-Rv; sequences in Table S1) for both *PSEN* and *S18* (Pliv08122.1, used as internal control), according to the manufacturer's instructions. Sequences were retrieved from a *P. lividus* cDNA library (http://octopus.obs-vlfr.fr). PCR was then performed using the GoTaq G2 Flexi DNA Polymerase kit (Promega) on equal amounts of cDNA with forward and reverse primers for either *PSEN* or *S18* rRNA (PSENpcr-Rv, PSENpcr-Fw, S18pcr-Rv and S18pcr-Fw; sequences in Table S1). PCR was performed with an initial denaturation step at 95°C for 30 s; 25 cycles of denaturation at 95°C for 30 s, annealing at 58°C for 30 s and extension at 72°C for 30 s; and a final extension at 72°C for 8 min. Aliquots (10–50%) of each amplicon were run on 2% agarose gels. Bands were quantified using ImageJ, normalized by comparison to *S18* levels and then expressed relative to the value determined in control embryos, which was arbitrarily taken as one.

Morpholinos and *PSEN* mRNA

The PSEN-MO, which targets a fragment of the 5′ region, and a standard negative control morpholino (ContMo), which targets a human β-globin intron containing a β-thalassemia mutation, were obtained from Gene Tools (Table S1).

The *PSEN* original sequence (Wt) in pBluescript II KS+, as described above, is targeted by the PSEN-MO but contains a stop codon sequence. We replaced this stop codon with the corresponding coding sequence found in the *S. purpuratus* PSEN, Sp-presenilin (SPU_006912) to obtain a new plasmid (Mut) containing a full coding sequence. The Wt plasmid was PCR amplified using Platinum SuperFi DNA Polymerase (Thermo Fisher Scientific) with the phosphorylated primers P-PSEN-Fw and P-PSEN-Rv (sequences in Table S1). The resulting PCR product was purified by NucleoSpin PCR Clean-up (Macherey Nagel) and self-ligated using T4 DNA ligase (Fermentas). Transformation was performed with One Shot TOP10 Chemically Competent *E. coli* (Invitrogen), following the manufacturer's protocol. Sequences of all plasmids were verified by Sanger sequencing before further use.

The corresponding morpholino-resistant plasmids (Wtr and Mutr) were built by overlapping PCR and by using the primers T7-Fw and MoR-Fw with the T3-Rv primer (sequences in Table S1). PCR was carried out with RedTaq PCR master mix (Sigma-Aldrich) and the Phusion High-Fidelity DNA Polymerase (Thermo Fisher Scientific), following the manufacturer's instructions. Subsequent PCR products were gel purified (NucleoSpin Gel and PCR Clean-up; Macherey Nagel) and used to perform overlapping PCR with the primers PSENpl-Fw and PSEN-Rv (sequences in Table S1) under the same experimental conditions (using a mix of RedTaq and Phusion High-Fidelity DNA Polymerase). The resulting PCR product was gel purified and cloned into pGEM-T Easy vector (Promega) following the manufacturer's protocol. The resulting plasmids were verified by Sanger sequencing, and one clone with T7 promoter sequence upstream of the modified PSEN sequence was kept as the PSEN-MoR plasmid.

The four plasmids (Wt, Wtr, Mut and Mutr) were used for *in vitro* transcription. All RNAs (WtRNA, WtrRNA, MutRNA and MutrRNA) were synthesized using the T7 mMessage mMachine (Ambion), as described by the manufacturer, using 1 µg of HindIII-linearized plasmid DNA matrix. After 2 h of incubation, the mixture was treated with turboDNAse (Ambion), and RNA was purified using phenol:chloroform then precipitated with isopropanol. RNA integrity and size were assessed on a 1% agarose gel, and RNA concentration was quantified using a Nanodrop. All sequences are listed in Tables S1, S2.

Injections

All injections were conducted as previously described (Houel-Renault et al., 2013). Fluorescent injected eggs were detected under a Nikon Eclipse TE300, equipped with a 20× or 40× Plan Fluor Nikon lens. A peptide corresponding to the endoproteolytic domain of PSEN (Cliv-Pep, sequence in Table S1) was synthesized (Proteogenix SAS, France). Antibodies, MO, mRNAs and the peptide were diluted in distilled water containing 2 mM carboxyfluorescein to visualize the injected eggs. We used a twofold dilution of the anti-CterPSEN antibody stock solution (200 µg/ml), up to a twofold dilution of the anti-NterPSEN antibody stock solution (1.6 mg/ml) and up to 100 µg/ml Cliv-pep. Morpholinos were injected at concentrations up to 150 µM. Increasing amounts of mRNAs (0.05–0.2 µg/µl), alone or together with the MO, were injected, as explained in the text.

Intracellular Ca^{2+} imaging

Ca_i was measured as described previously (Ciapa and Philippe, 2013) by using 10 kDa Fura-2 dextran (Molecular Probes). Results are shown as the ratio of Fura-2 (340/380 nm excitation ratio).

Acknowledgements

We thank I. Arnone and M. Perillo for their helpful comments during this study and Michael Schubert for his advice concerning evolution data.

Competing interests

The authors declare no competing or financial interests.

Author contributions

Conceptualization: B.C.; Methodology: O.B., L.P.-C., V.A., B.C.; Software: B.C.; Validation: B.C.; Formal analysis: L.P.-C., V.A., B.C.; Investigation: O.B., L.P.-C., V.A., B.C.; Resources: B.C.; Data curation: B.C.; Writing - original draft: B.C.; Writing - review & editing: O.B., V.A., B.C.; Visualization: B.C.; Supervision: B.C.; Project administration: B.C.; Funding acquisition: B.C.

Funding

This research was funded by the Centre National de la Recherche Scientifique.

References

Annunziata, R., Perillo, M., Andrikou, C., Cole, A. G., Martinez, P. and Arnone, M. I. (2014). Pattern and process during sea urchin gut morphogenesis: the regulatory landscape. *Genesis* **52**, 251-268. doi:10.1002/dvg.22738

Area-Gomez, E., de Groof, A. J. C., Boldogh, I., Bird, T. D., Gibson, G. E., Koehler, C. M., Yu, W. H., Duff, K. E., Yaffe, M. P., Pon, L. A. et al. (2009).

Presenilins Are Enriched in Endoplasmic Reticulum Membranes Associated with Mitochondria. *Am. J. Pathol.* **175**, 1810-1816. doi:10.2353/ajpath.2009.090219
Beher, D., Wrigley, J. D., Nadin, A., Evin, G., Masters, C. L., Harrison, T., Castro, J. L. and Shearman, M. S. (2001). Pharmacological knock-down of the presenilin 1 heterodimer by a novel γ-secretase inhibitor: implications for presenilin biology. *J. Biol. Chem.* **276**, 45394-45402. doi:10.1074/jbc.M103075200
Benson, R. A., Lowrey, J. A., Lamb, J. R. and Howie, S. E. (2004). The Notch and Sonic hedgehog signalling pathways in immunity. *Mol. Immunol.* **41**, 715-725. doi:10.1016/j.molimm.2004.04.017
Ben-Tabou de-Leon, S. (2016). Robustness and Accuracy in Sea Urchin Developmental Gene Regulatory Networks. *Front. Genet.* **7**, 16-27. doi:10.3389/fgene.2016.00016
Bray, S. J. (2016). Notch signalling in context. *Nat. Rev. Mol. Cell. Biol.* **17**, 722-735. doi:10.1038/nrm.2016.94
Bronchain, O., Jdey, W., Caraty, L. and Ciapa, B. (2017). Role of Mad2 expression during the early development of the sea urchin. *Int. J. Dev. Biol.* **61**, 451-457. doi:10.1387/ijdb.170053bc
Brunkan, A. L., Martinez, M., Walker, E. S. and Goate, A. M. (2005). Presenilin endoproteolysis is an intramolecular cleavage. *Mol. Cell. Neurosci.* **29**, 65-73. doi:10.1016/j.mcn.2004.12.012
Bryja, V., Červenka, I. and Čajánek, L. (2017). The connections of Wnt pathway components with cell cycle and centrosome: side effects or a hidden logic? *Crit. Rev. Biochem. Mol. Biol.* **52**, 614-637 doi:10.1080/10409238.2017.1350135
Buckley, K. M. and Rast, J. P. (2017). An Organismal Model for Gene Regulatory Networks in the Gut-Associated Immune Response. *Front. Immunol.* **8**, 1297. doi:10.3389/fimmu.2017.01297
Burke, R. D., Angerer, L. M., Elphick, M. R., Humphrey, G. W., Yaguchi, S., Kiyama, T., Liang, S., Mu, X., Agca, C., Klein, W. H. et al. (2006). A genomic view of the sea urchin nervous system. *Dev. Biol.* **300**, 434-460. doi:10.1016/j.ydbio.2006.08.007
Burke, R. D., Moller, D. J., Krupke, O. A. and Taylor, V. J. (2014). Sea urchin neural development and the metazoan paradigm of neurogenesis. *Genesis* **52**, 208-221. doi:10.1002/dvg.22750
Campbell, W. A., Iskandar, M. K., Reed, M. L. and Xia, W. (2002). Endoproteolysis of presenilin *in vitro*: inhibition by γ-secretase inhibitors. *Biochemistry* **41**, 3372-3379. doi:10.1021/bi015810h
Ciapa, B. and Philippe, L. (2013). Intracellular and Extracellular pH and Ca are bound to control mitosis in the early Sea Urchin Embryo via ERK and MPF Activities. *PLoS ONE* **8**, e66113. doi:10.1371/journal.pone.0066113
Colin, A. M. and Hille, M. B. (1986). Injected mRNA does not increase protein synthesis in unfertilized, fertilized, or ammonia-activated sea urchin eggs. *Dev. Biol.* **115**, 184-192. doi:10.1016/0012-1606(86)90239-3
Collu, G. M., Hidalgo-Sastre, A. and Brennan, K. (2014). Wnt-Notch signalling crosstalk in development and disease. *Cell. Mol. Life Sci.* **71**, 3553-3567. doi:10.1007/s00018-014-1644-x
Contakos, S. P., Gaydos, C. M., Pfeil, E. C. and McLaughlin, K. A. (2005). Subdividing the embryo: a role for Notch signaling during germ layer patterning in Xenopus laevis. *Dev. Biol.* **288**, 294-307. doi:10.1016/j.ydbio.2005.09.015
Costache, V., McDougall, A. and Dumollard, R. (2014). Cell cycle arrest and activation of development in marine invertebrate deuterostomes. *Biochem. Biophys. Res. Commun.* **450**, 1175-1181. doi:10.1016/j.bbrc.2014.03.155
De Strooper, B., Beullens, M., Contreras, B., Levesque, L., Craessaerts, K., Cordell, B., Moechars, D., Bollen, M., Fraser, P., George-Hyslop, P. S. et al. (1997). Phosphorylation, subcellular localization, and membrane orientation of the Alzheimer's disease-associated presenilins. *J. Biol. Chem.* **272**, 3590-3598. doi:10.1074/jbc.272.6.3590
Dehvari, N., Isacsson, O., Winblad, B., Cedazo-Minguez, A. and Cowburn, R. F. (2008). Presenilin regulates extracellular regulated kinase (Erk) activity by a protein kinase C alpha dependent mechanism. *Neurosci. Lett.* **436**, 77-80. doi:10.1016/j.neulet.2008.02.063
Duboc, V., Röttinger, E., Besnardeau, L. and Lepage, T. (2004). Nodal and BMP2/4 signaling organizes the oral-aboral axis of the sea urchin embryo. *Dev. Cell* **6**, 397-410. doi:10.1016/s1534-5807(04)00056-5
Duggan, S. P. and McCarthy, J. V. (2016). Beyond γ-secretase activity: The multifunctional nature of presenilins in cell signalling pathways. *Cell. Signal.*. **28**, 1-11. doi:10.1016/j.cellsig.2015.10.006
Escamilla-Ayala, A. A., Sannerud, R., Mondin, M., Poersch, K., Vermeire, W., Paparelli, L., Berlage, C., Koenig, M., Chavez-Gutierrez, L. and Ulbrich, M. H. (2020). Super-resolution microscopy reveals majorly mono- and dimeric presenilin1/γ-secretase at the cell surface. *eLife* **9**, e56679. doi:10.7554/eLife.56679
Floc'hlay, S., Molina, M. D., Hernandez, C., Haillot, E., Thomas-Chollier, M., Lepage, T. and Thieffry, D. (2021). Deciphering and modelling the TGF-β signalling interplays specifying the dorsal-ventral axis of the sea urchin embryo. *Development* **148**, dev189944.
Fuss, B. and Hoch, M. (2002). Notch signaling controls cell fate specification along the dorsoventral axis of the Drosophila gut. *Curr. Biol.* **12**, 171-179. doi:10.1016/s0960-9822(02)00653-x
Garner, S., Zysk, I., Byrne, G., Kramer, M., Moller, D., Taylor, V. and Burke, R. D. (2016). Neurogenesis in sea urchin embryos and the diversity of deuterostome neurogenic mechanisms. *Development* **143**, 286-297.
Guo, Y., Livne-Bar, I., Zhou, L. and Boulianne, G. L. (1999). Drosophila presenilin is required for neuronal differentiation and affects notch subcellular localization and signaling. *J. Neurosci.* **19**, 8435-8842. doi:10.1523/JNEUROSCI.19-19-08435.1999
Haapasalo, A. and Kovacs, D. M. (2011). The many substrates of presenilin/γ-secretase. *J. Alzheimer's Dis.* **25**, 3-28. doi:10.3233/JAD-2011-101065
Herreman, A., Hartmann, D., Annaert, W., Saftig, P., Craessaerts, K., Serneels, L., Umans, L., Schrijvers, V., Checler, F. and Vanderstichele, H. (1999). Presenilin 2 deficiency causes a mild pulmonary phenotype and no changes in amyloid precursor protein processing but enhances the embryonic lethal phenotype of presenilin 1 deficiency. *Proc. Natl. Acad. Sci. USA* **96**, 11872-11877. doi:10.1073/pnas.96.21.11872
Hinman, V. F. and Burke, R. D. (2018). Embryonic neurogenesis in echinoderms. *Wiley Interdiscip. Rev. Dev. Biol.* **7**, e316. doi:10.1002/wdev.316
Ho, A. and Shen, J. (2011). Presenilins in synaptic function and disease. *Trends Mol. Med.* **17**, 617-624. doi:10.1016/j.molmed.2011.06.002
Holland, L. Z., Rached, L. A., Tamme, R., Holland, N. D., Kortschak, D., Inoko, H., Shiina, T., Burgtorf, C. and Lardelli, M. (2001). Characterization and developmental expression of the amphioxus homolog of Notch (AmphiNotch): evolutionary conservation of multiple expression domains in amphioxus and vertebrates. *Dev. Biol.* **232**, 493-507. doi:10.1006/dbio.2001.0160
Hollands, C., Bartolotti, N. and Lazarov, O. (2016). Alzheimer's Disease and Hippocampal Adult Neurogenesis; Exploring Shared Mechanisms. *Front. Neurosci.* **10**, 178-201. doi:10.3389/fnins.2016.00178
Honarnejad, K. and Herms, J. (2012). Presenilins: role in calcium homeostasis. *Int. J. Biochem. Cell Biol.* **44**, 1983-1986. doi:10.1016/j.biocel.2012.07.019
Houel-Renault, L., Philippe, L., Piquemal, M. and Ciapa, B. (2013). Autophagy is used as a survival program in unfertilized sea urchin eggs that are destined to die by apoptosis after inactivation of MAPK1/3 (ERK2/1). *Autophagy* **9**, 1527-1539. doi:10.4161/auto.25712
Khan, A. A., Ali, R. H. and Mirza, B. (2020). Evolutionary history of alzheimer disease-causing protein family presenilins with pathological implications. *J. Mol. Evol.* **88**, 674-688. doi:10.1007/s00239-020-09966-w
Kikuchi, Y., Verkade, H., Reiter, J. F., Kim, C. H., Chitnis, A. B., Kuroiwa, A. and Stainier, D. Y. R. (2004). Notch signaling can regulate endoderm formation in zebrafish. *Dev. Dyn.* **229**, 756-762. doi:10.1002/dvdy.10483
Kong, J. H., Yang, L., Dessaud, E., Chuang, K., Moore, D. M., Rohatgi, R., Briscoe, J. and Novitch, B. G. (2015). Notch activity modulates the responsiveness of neural progenitors to sonic hedgehog signaling. *Dev. Cell.* **33**, 373-387. doi:10.1016/j.devcel.2015.03.005
Kumar, M., Pushpa, K. and Mylavarapu, S. V. (2015). Splitting the cell, building the organism: Mechanisms of cell division in metazoan embryos. *IUBMB Life* **67**, 575-587. doi:10.1002/iub.1404
Lanoiselée, H. M., Nicolas, G., Wallon, D., Rovelet-Lecrux, A., Lacour, M., Rousseau, S., Richard, A.-C., Pasquier, F., Rollin-Sillaire, A. and Martinaud, O. (2017). APP, PSEN1, and PSEN2 mutations in early-onset Alzheimer disease: A genetic screening study of familial and sporadic cases. *PLoS Med.* **14**, e1002270. doi:10.1371/journal.pmed.1002270
Liu, J. A. and Ngan, E. S. (2014). Hedgehog and Notch signaling in enteric nervous system development. *NeuroSignals* **22**, 1-13. doi:10.1159/000356305
Ludtmann, M. H., Otto, G. P., Schilde, C., Chen, Z. H., Allan, C. Y., Brace, S., Beesley, P. W., Kimmel, A. R., Fisher, P., Killick, R. et al. (2014). An ancestral non-proteolytic role for presenilin proteins in multicellular development of the social amoeba Dictyostelium discoideum. *J. Cell. Sci.* **127**, 1576-1584.
Materna, S. C., Swartz, S. Z. and Smith, J. (2013). Notch and Nodal control forkhead factor expression in the specification of multipotent progenitors in sea urchin. *Development* **140**, 1796-1806. doi:10.1242/dev.091157
Mathews, P. M., Cataldo, A. M., Kao, B. H., Rudnicki, A. G., Qin, X., Yang, J. L., Jiang, Y., Picciano, M., Hulette, C. and Lippa, C. F. (2000). Brain expression of presenilins in sporadic and early-onset, familial Alzheimer's disease. *Mol. Med.* **6**, 878-891. doi:10.1007/BF03401825
Matsuda, Y., Wakamatsu, Y., Kohyama, J., Okano, H., Fukuda, K. and Yasugi, S. (2005). Notch signaling functions as a binary switch for the determination of glandular and luminal fates of endodermal epithelium during chicken stomach development. *Development* **132**, 2783-2793. doi:10.1242/dev.01853
McClay, D. R. (2011). Evolutionary crossroads in developmental biology: sea urchins. *Development* **138**, 2639-2648. doi:10.1242/dev.048967
Morris, R. L. and Vacquier, V. D. (2019). Sea urchin embryonic cilia. *Methods Cell Biol.*. **150**, 235-250 doi:10.1016/bs.mcb.2018.11.016
Nakajima, Y., Kaneko, H., Murray, G. and Burke, R. D. (2004). Divergent patterns of neural development in larval echinoids and asteroids. *Evol. Dev.* **6**, 95-104. doi:10.1111/j.1525-142x.2004.04011.x
Ohguro, Y. L., Takata, H. and Kominami, T. (2011). Involvement of Delta and Nodal signals in the specification process of five types of secondary mesenchyme cells in embryo of the sea urchin, Hemicentrotus pulcherrimus. *Dev. Growth Differ.* **53**, 110-123. doi:10.1111/j.1440-169X.2010.01233.x

Oikawa, N. and Walter, J. (2019). Presenilins and γ-Secretase in Membrane Proteostasis. *Cells* **8**, 209-241. doi:10.3390/cells8030209

Otto, G. P., Sharma, D. and Williams, R. S. (2016). Non-Catalytic Roles of Presenilin Throughout Evolution. *J. Alzheimers Dis.* **52**, 1177-1187. doi:10.3233/JAD-150940

Pack-Chung, E., Meyers, M. B., Pettingell, W. P., Moir, R. D., Brownawell, A. M., Cheng, I., Tanzi, R. E. and Kim, T. W. (2000). Presenilin 2 interacts with sorcin, a modulator of the ryanodine receptor. *J. Biol. Chem.* **275**, 14440-14445. doi:10.1074/jbc.M909882199

Parks, A. L. and Curtis, D. (2007). Presenilin diversifies its portfolio. *Trends Genet.*. **23**, 140-150. doi:10.1016/j.tig.2007.01.008

Perillo, M., Wang, Y. J., Leach, S. D. and Arnone, M. I. (2016). A pancreatic exocrine-like cell regulatory circuit operating in the upper stomach of the sea urchin Strongylocentrotus purpuratus larva. *BMC Evol. Biol.* **16**, 117. doi:10.1186/s12862-016-0686-0

Philippe, L., Tosca, L., Zhang, W. L., Piquemal, M. and Ciapa, B. (2014). Different routes lead to apoptosis in unfertilized sea urchin eggs. *Apoptosis*. **19**, 436-450. doi:10.1007/s10495-013-0950-3

Prüßing, K., Voigt, A. and Schulz, J. B. (2013). Drosophila melanogaster as a model organism for Alzheimer's disease. *Mol. Neurodegener.* **8**, 35-61. doi:10.1186/1750-1326-8-35

Sarasija, S. and Norman, K. R. (2015). A γ-secretase independent role for presenilin in calcium homeostasis impacts mitochondrial function and morphology in Caenorhabditis elegans. *Genetics* **201**, 1453-1466. doi:10.1534/genetics.115.182808

Schröder, N. and Gossler, A. (2002). Expression of Notch pathway components in fetal and adult mouse small intestine. *Gene Expr. Patterns* **2**, 247-250. doi:10.1016/s1567-133x(02)00060-1

Sethi, A. J., Wikramanayake, R. M., Angerer, R. C., Range, R. C. and Angerer, L. M. (2012). Sequential signaling crosstalk regulates endomesoderm segregation in sea urchin embryos. *Science* **335**, 590-593. doi:10.1126/science.1212867

Sherwood, D. R. and McClay, D. R. (1999). LvNotch signaling mediates secondary mesenchyme specification in the sea urchin embryo. *Development* **126**, 1703-1713. doi:10.1242/dev.126.8.1703

Sherwood, D. R. and McClay, D. R. (2001). LvNotch signaling plays a dual role in regulating the position of the ectoderm-endoderm boundary in the sea urchin embryo. *Development* **128**, 2221-2232. doi:10.1242/dev.128.12.2221

Slota, L. A., Miranda, E., Peskin, B. and McClay, D. R. (2020). Developmental origin of peripheral ciliary band neurons in the sea urchin embryo. *Dev. Biol.* **459**, 72-78. doi:10.1016/j.ydbio.2019.12.011

Su, Y. H., Chen, Y. C., Ting, H. C., Fan, T. P., Lin, C. Y., Wang, K. T. and Yu, Jr., K. (2019). BMP controls dorsoventral and neural patterning in indirect-developing hemichordates providing insight into a possible origin of chordates. *Proc. Natl. Acad. Sci. USA* **116**, 12925-12932. doi:10.1073/pnas.1901919116

Tesco, G., Kim, T. W., Diehlmann, A., Beyreuther, K. and Tanzi, R. E. (1998). Abrogation of the presenilin 1/β-catenin interaction and preservation of the heterodimeric presenilin 1 complex following caspase activation. *J. Biol. Chem.* **273**, 33909-33914. doi:10.1074/jbc.273.51.33909

Thinakaran, G., Borchelt, D. R., Lee, M. K., Slunt, H. H., Spitzer, L., Kim, G., Ratovitsky, T., Davenport, F., Nordstedt, C., Seeger, M. et al. (1996). Endoproteolysis of presenilin 1 and accumulation of processed derivatives in vivo. *Neuron* **17**, 181-190. doi:10.1016/s0896-6273(00)80291-3

Tosca, L., Glass, R., Bronchain, O., Philippe, L. and Ciapa, B. (2012). PLCgamma, G-protein of the Gαq type and cADPr pathway are associated to trigger the fertilization Ca^{2+} signal in the sea urchin egg. *Cell Calcium* **52**, 388-396. doi:10.1016/j.ceca.2012.06.006

Tse, K. H. and Herrup, K. (2017). Re-imagining Alzheimer's disease – the diminishing importance of amyloid and a glimpse of what lies ahead. *J. Neurochem.* **143**, 432-444. doi:10.1111/jnc.14079

Wahi, K., Bochter, M. S. and Cole, S. E. (2016). The many roles of Notch signaling during vertebrate somitogenesis. *Semin. Cell. Dev. Biol.* **49**, 68-75. doi:10.1016/j.semcdb.2014.11.010

Walton, K. D., Croce, J. C., Glenn, T. D., Wu, S. Y. and McClay, D. R. (2006). Genomics and expression profiles of the Hedgehog and Notch signaling pathways in sea urchin development. *Dev. Biol.* **300**, 153-164. doi:10.1016/j.ydbio.2006.08.064

Warner, J. F., McCarthy, A. M., Morris, R. L. and McClay, D. R. (2014). Hedgehog signaling requires motile cilia in the sea urchin. *Mol. Bio.l Evol.* **31**, 18-22. doi:10.1093/molbev/mst176

Wei, Z., Angerer, R. C. and Angerer, L. M. (2011). Direct development of neurons within foregut endoderm of sea urchin embryos. *Proc. Natl. Acad. Sci. USA* **108**, 9143-9147. doi:10.1073/pnas.1018513108

Whitaker, M. (2008). Calcium signalling in early embryos. *Philos. Trans. R. Soc. Lond. B. Biol. Sci.* **363**, 1401-1418. doi:10.1098/rstb.2008.2259

Wolfe, M. S. (2019). Dysfunctional γ-Secretase in Familial Alzheimer's Disease. *Neurochem. Res.* **44**, 5-11. doi:10.1007/s11064-018-2511-1

Wong, P. C., Zheng, H., Chen, H., Becher, M. W., Sirinathsinghji, D. J., Trumbauer, M. E., Chen, H. Y., Price, D. L., Van der Ploeg, L. H. T. and Sisodia, S. S. (1997). Presenilin 1 is required for Notch1 and Dll1 expression in the paraxial mesoderm. *Nature* **387**, 288-292. doi:10.1038/387288a0

Wood, N. J., Mattiello, T., Rowe, M. L., Ward, L., Perillo, M., Arnone, M. I., Elphick, M. R. and Oliveri, P. (2018). Neuropeptidergic Systems in Pluteus Larvae of the Sea Urchin Strongylocentrotus purpuratus: Neurochemical Complexity in a 'Simple' Nervous System. *Front. Endocrinol. (Lausanne)* **9**, 628. doi:10.3389/fendo.2018.00628

Xia, W. (2019). γ-Secretase and its modulators: Twenty years and beyond. *Neurosci. Lett.* **701**, 162-169. doi:10.1016/j.neulet.2019.02.011

Yaguchi, J., Angerer, L. M., Inaba, K. and Yaguchi, S. (2012). Zinc finger homeobox is required for the differentiation of serotonergic neurons in the sea urchin embryo. *Dev. Biol.* **363**, 74-83. doi:10.1016/j.ydbio.2011.12.024

Zhang, W. L., Huitorel, P., Glass, R., Fernandez-Serra, M., Arnone, M. I., Chiri, S., Picard, A. and Ciapa, B. (2005). A MAPK pathway is involved in the control of mitosis after fertilization of the sea urchin egg. *Dev. Biol.* **282**, 192-206. doi:10.1016/j.ydbio.2005.03.008

Zhang, R., Engler, A. and Taylor, V. (2018). Notch: an interactive player in neurogenesis and disease. *Cell Tissue Res.*. **371**, 73-89. doi:10.1007/s00441-017-2641-9